Supplemental Data

Heterologous phosphorylation-induced formation of a stability lock permits regulation of inactive receptors by β-arrestins

András D. Tóth[‡,1], Susanne Prokop[‡,1], Pál Gyombolai[‡,§], Péter Várnai[‡,§], András Balla[‡,§], Vsevolod V. Gurevich[¶], László Hunyady[‡,§,2], Gábor Turu[‡,§]

From the [‡]Department of Physiology, Faculty of Medicine, Semmelweis University, Budapest, Hungary,
the [§]MTA-SE Laboratory of Molecular Physiology, Hungarian Academy of Sciences and Semmelweis University, Budapest, Hungary,
and the [¶]Department of Pharmacology, Vanderbilt University, Nashville, TN, USA
[1] These authors contributed equally to this work.
[2] To whom correspondence should be addressed: László Hunyady, Address: Department of Physiology, Faculty of Medicine, Semmelweis University, H-1428 Budapest, P.O. Box 2, Hungary. Tel.: +36 1 266
9180; fax: +36 1 266 6504. Electronic address: hunyady.laszlo@med.semmelweis-univ.hu

Running title: Heterologous regulation of inactive receptors via β-arrestin

Included figure supplements:

Figure S1

Figure S2

Figure S3

Figure S4

Figure S5

Figure S1

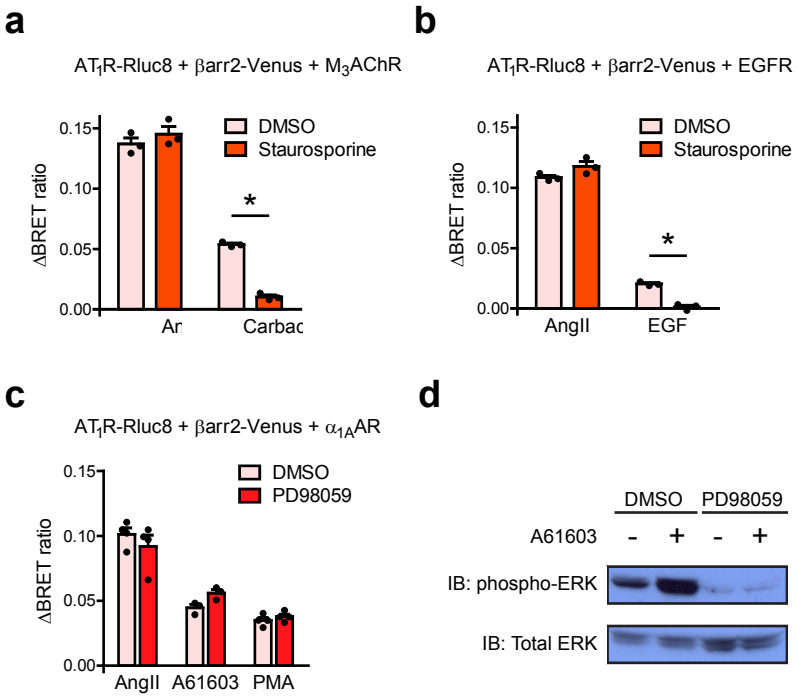

Figure S1. Stimulation of a $G_{q/11}$-coupled receptor or EGFR induces PKC-dependent binding between AT_1R and β-arrestin2

a and **b**, Intermolecular BRET was measured in cells co-expressing AT_1R-Rluc8, β-arrestin2-Venus and M_3AChR (**a**) or EGFR (**b**), as indicated. After 30-minute pretreatment with vehicle (DMSO) or 500 nM staurosporine, the cells were stimulated with 100 nM AngII, (**a**-**b**) 10 μM carbachol (**a**) or 100 ng/ml EGF (**b**).

c, Cells co-expressing AT_1R-Rluc8, β-arrestin2-Venus and untagged $\alpha_{1A}AR$ were pretreated with vehicle (DMSO) or MEK1 inhibitor PD98059 (100 μM) and stimulated with AngII, 100 nM PMA or $\alpha_{1A}AR$ specific agonist A61603 (1 μM), and intermolecular BRET was measured. The average BRET ratio changes are presented in scatter dot plots with columns (mean+s.e.m.) of independent biological replicates (n=3-4). *,P<0.05, pretreatment significantly inhibits the effect of the stimulus, as revealed by Two-Way ANOVA.

d, Immunoblot analysis of ERK phosphorylation. The day before transfection HEK 293T cells were plated on poly-L-lysine coated 6-well plates. The cells were transfected with cDNA encoding $\alpha_{1A}AR$. 24 hours later, the cells were serum-starved for 2 hours, pretreated with DMSO or 100 μM PD98059 for 30 minutes, then stimulated with 1 μM A61603 for 5 minutes. Representative blots of 3 independent experiments are shown.

Figure S2

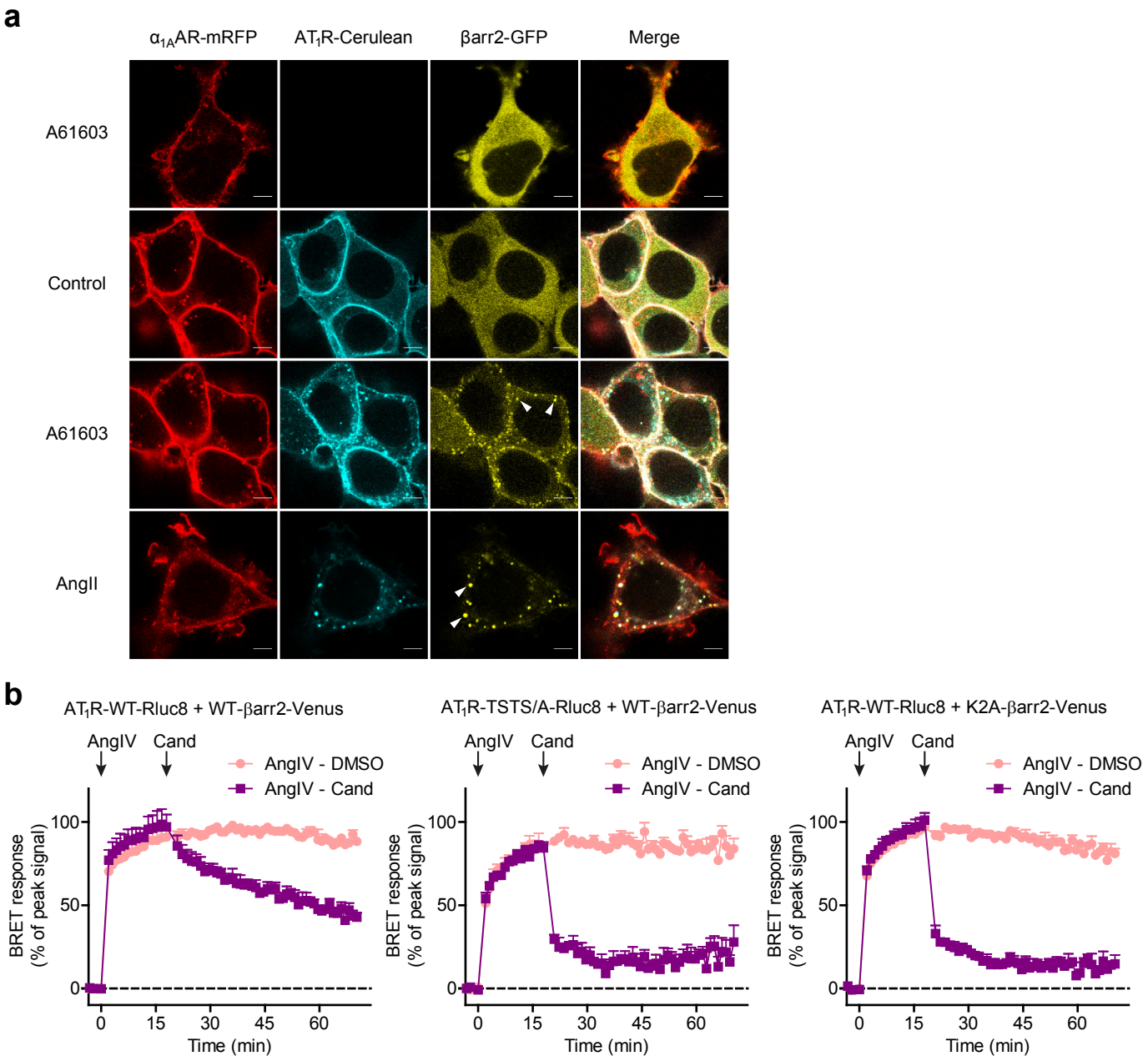

Figure S2.

a, α_{1A}AR activation triggers β-arrestin2 recruitment to AT_1R, followed by their co-internalization

HEK 293T cells co-expressing α_{1A}AR-mRFP, β-arrestin2-GFP with or without (top) AT_1R-Cerulean were visualized with confocal microscope. Images were taken before (control) and after 20 minutes of stimulation with 1 μM α_{1A}AR agonist A61603 or AngII, fluorescence was recorded by confocal microscopy. Representative images from 3 independent experiments are shown. Arrowheads mark endosomal-localized β-arrestin2-GFP, which were present after A61603 treatment only in the case of AT1R-Cerulean co-expression (third row). Scale bars represent 5 μm.

b, Disruption of the stabilization lock accelerates the β-arrestin2 dissociation from inactive AT_1R

Cells were co-transfected with WT or TSTS/A-mutant AT_1R-Rluc8 and WT- or K2A-β-arrestin2-Venus, as indicated, and with dominant-negative dynamin to inhibit receptor internalization. β-arrestin2 binding to AT_1R was monitored using BRET. The interaction was induced with 10 μM low-affinity agonist angiotensin IV (AngIV) treatment, then AngIV was displaced by addition of 10 μM high-affinity competitive antagonist candesartan (Cand). BRET ratio dropped faster in the case of TSTS/A- and K2A-mutations, showing that the stability of the interaction is decreased in the absence of stability lock formation. Values are presented as percentage of the peak AngIV-induced signal in each experiment and each set-up as mean+s.e.m. of 3 independent biological replicates, each experiment was performed in duplicate.

Figure S3

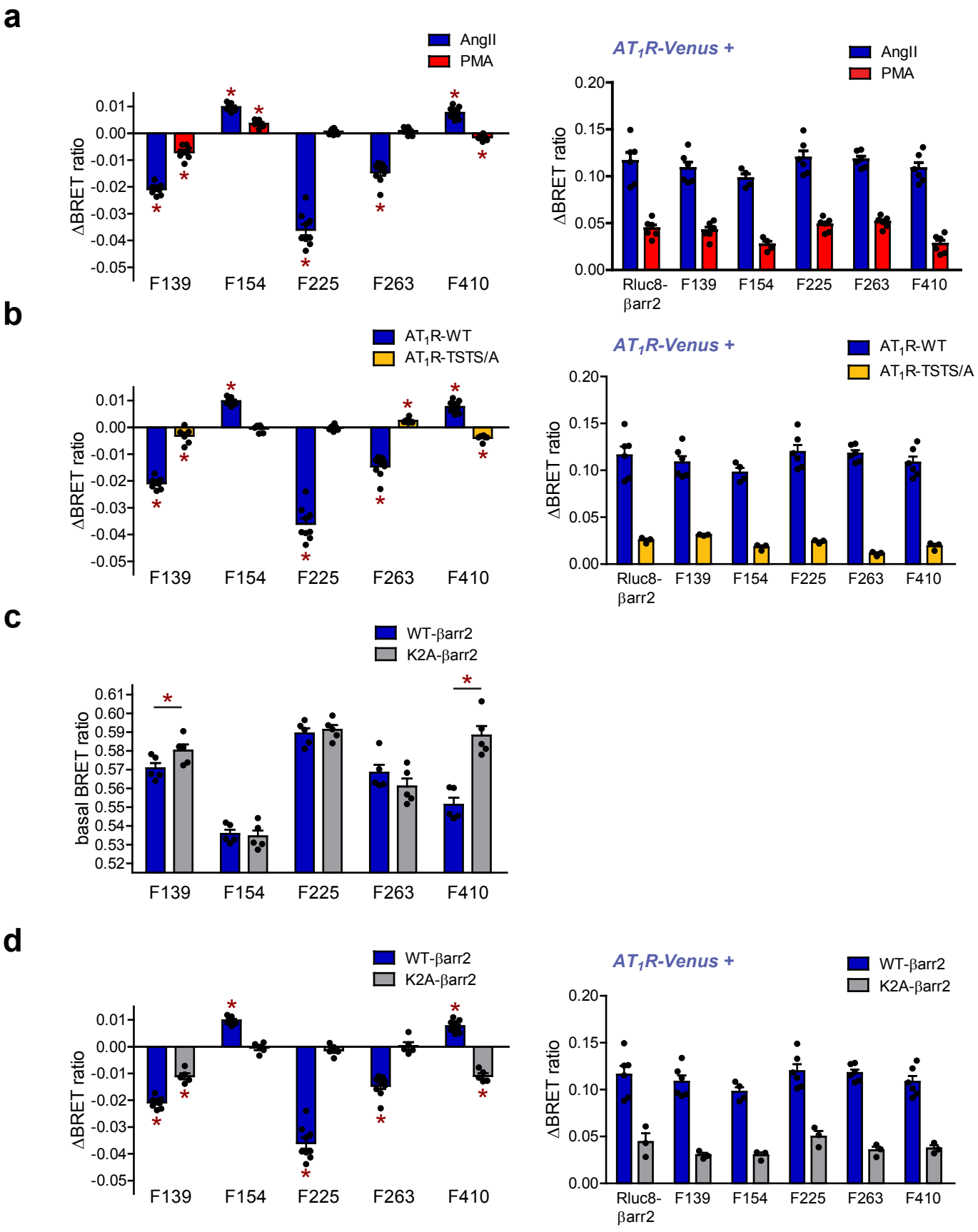

Figure S3 continued on next page

Figure S3 continued

Figure S3. Intra- and intermolecular BRET signals detected with FlAsH biosensors

a,b,d left panels, Stimulus-induced intramolecular (conformational) BRET changes of FlAsH dye-labelled biosensors were detected in cells co-expressing wild type untagged AT_1R and wild type biosensors (**a**), AT_1R-TSTS/A and wild type biosensors (**b**), or wild type AT_1R and FlAsH biosensors harboring K2A mutation (**d**).

a,b,d right panels, Intermolecular (interactional) BRET changes between AT_1R-Venus and FlAsH biosensors (**a**), AT_1R-TSTS/A-Venus and wild type sensors (**b**), AT_1R-Venus und K2A-mutant FlAsH biosensors (**c**). AngII (**a**,**b**,**c**) or PMA (**a**) were used as stimuli. Average BRET ratio changes are shown in scatter dot plots with columns (mean+s.e.m.) of independent biological replicates, n=5-10 (the exact n values are presented in the figure legends of Fig. 3 and 4). *,P<0.05, significant difference compared to vehicle-stimulated control, analyzed with paired two-tailed two-sample t-test. There was no significant difference in the recruitment of Rluc8-β-arrestin2 and the FlAsH sensors to AT_1R upon AngII treatment (analyzed with One-Way ANOVA with Bonferroni post hoc-test).

c, Basal intramolecular (conformational) BRET ratios measured in cells co-expressing untagged AT_1R and wild type or K2A-mutant FlAsH biosensors labelled with FlAsH dye. n=5, scatter dot plots with columns (mean+s.e.m.) are presented, *,P<0.05, analyzed with One-Way ANOVA (repeated measures) with Bonferroni post hoc-test.

Figure S4

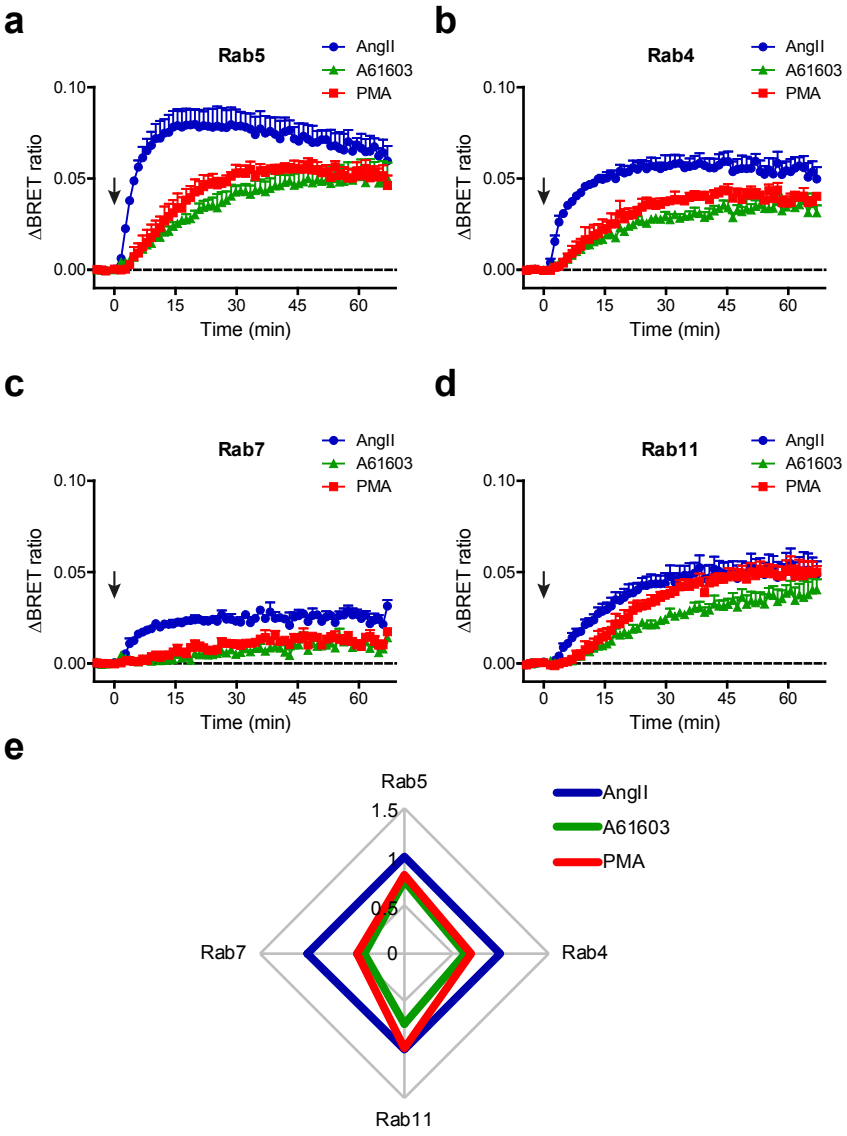

Figure S4. Stimulation of α_{1A}AR induces distinct intracellular redistribution of AT_1R

Cells were co-transfected with plasmids encoding AT_1R-Rluc8, Venus-tagged Rab construct (**a**, Rab5; **b**, Rab4; **c**, Rab7; **d**, Rab11), untagged α_{1A}AR and untagged β-arrestin2. AT_1R agonist AngII, PKC-activator PMA, or α_{1A}AR agonist A61603 were used as stimuli. The kinetics of BRET ratio changes are shown as mean+s.e.m in **a**-**d** panels.

e, Patterns of intracellular redistribution of AT_1R. BRET ratio changes after 60±2-minute stimulation were normalized to the AngII-induced changes, and the values are shown in radial diagram. α_{1A}AR stimulation and PMA treatment induced similar patterns of BRET ratio changes, which are distinct from that of AngII.

Figure S5

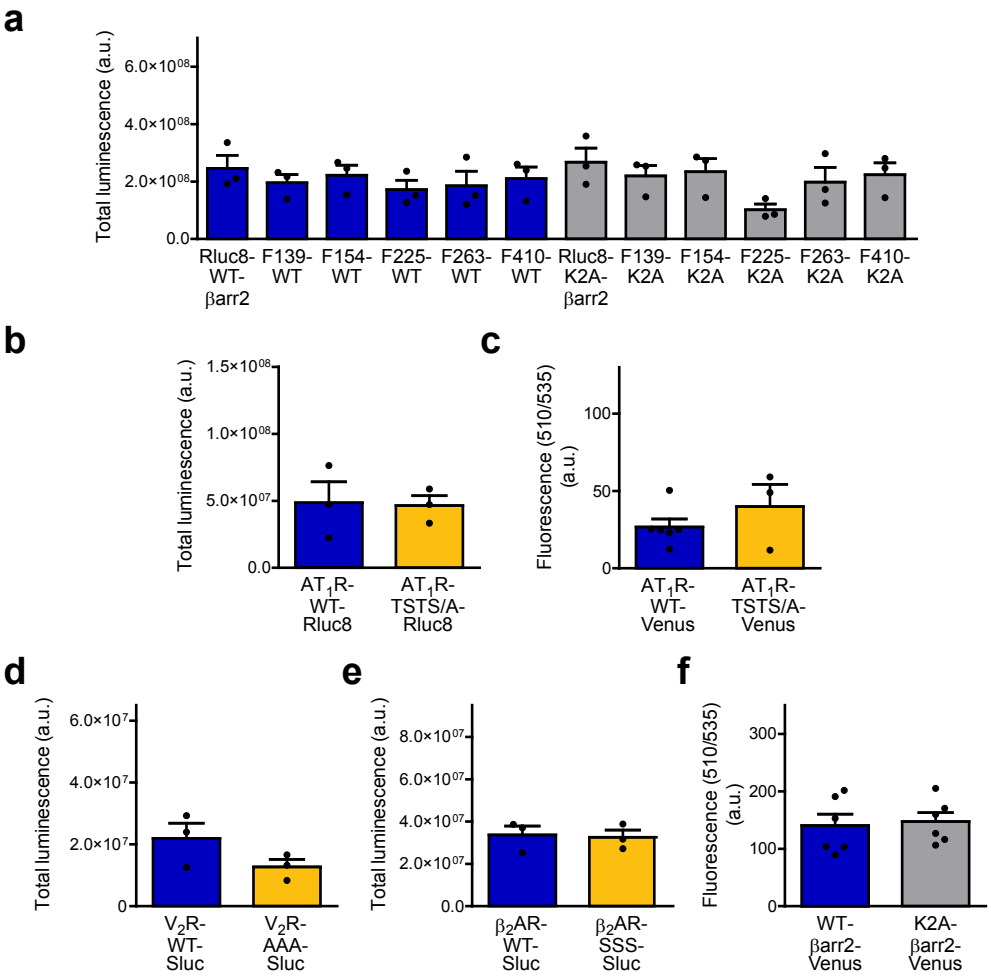

Figure S5. Expression levels of the wild type and mutant BRET constructs used in this study

a, Expression of the FlAsH-BRET β-arrestin2 biosensors. Total luminescence was determined before stimulation in AT_1R-Venus and biosensor co-expressing cells. There was no significant difference in the luminescence of the biosensors compared to Rluc8-WT-β-arrestin2, analyzed with One-Way ANOVA (repeated measures) with Bonferroni post hoc-test. (n=3, biological replicates).

b,**d**,**e**, Expression of the donor-tagged mutant receptors. Cells were transfected with wild type or mutant AT_1R-Rluc8 (**b**), V_2R-Sluc (**d**) and β_2AR-Sluc (**e**), as indicated, and total luminescence was measured. (n=3, experiments were performed in quadruplicate).

c,**f**, Expression of the acceptor-tagged wild type and mutant AT_1R and β-arrestin2. The fluorescence of wild type and TSTS/A mutant AT_1R-Venus was measured in receptor and wild type FlAsH-BRET β-arrestin2 biosensor co-expressing cells (**c**) (n=6 and n=3, respectively, biological replicates). The β-arrestin2-Venus fluorescence was measured in β_2AR-Sluc (WT and SSS mutant, n=3-3, respectively) co-expressing cells (data from Figure 4b, left panel) (**f**). Scatter dot plots with columns (mean+s.e.m.) are shown. There was no significant difference in the expression of the wild type and mutant proteins, analyzed with Student's two-sample t-test.